

An Instantaneous Power Balancing Control With Power Factor Correction for Single-Stage Three-Phase AC-DC Converters

Mojtaba Forouzesh
Department of Electrical and Computer
Engineering
Queen's University
Kingston, ON, Canada
m.forouzesh@queensu.ca

Yan-Fei Liu, *Fellow, IEEE*
Department of Electrical and Computer
Engineering
Queen's University
Kingston, ON, Canada
yanfei.liu@queensu.ca

Paresh C. Sen, *Life Fellow, IEEE*
Department of Electrical and Computer
Engineering
Queen's University
Kingston, ON, Canada
senp@queensu.ca

Abstract— A novel inner control loop for phase-modular three-phase single-stage rectifiers is proposed in this paper to achieve both power factor correction and power balancing at the same time. The power balancing control is critical in single-stage three-phase AC-DC converters as any small voltage imbalance in the three-phase voltages reflects into the output in the form of double line frequency voltage ripple that will prohibit electrolytic capacitor less implementation. The proposed instantaneous power balancing control approach is implemented on a single-stage LLC-based three-phase AC-DC converter. Balanced and unbalanced three-phase systems are considered in computer simulations to verify the effectiveness of the proposed method in removing line frequency power decoupling from the output capacitor. Moreover, a harmonic polluted three-phase voltage is also considered in the simulation to further verify the performance under non-ideal grid conditions. Furthermore, experimental results of a digitally controlled laboratory prototype validated unity power factor correction and the effectiveness of the proposed power balancing control method in rejecting line frequency output ripple in the presence of three-phase voltage imbalances.

Keywords— *Three-phase AC-DC converters, instantaneous power balancing, unbalanced three-phase, phase-modular rectifier, power factor correction (PFC), single-stage LLC.*

I. INTRODUCTION

When high power conversion from the AC mains to a DC load is required, three-phase rectifiers are the preferred solution. For example, high-power three-phase rectifiers are required in a 400 V data center power distribution system as well as in electric vehicle charging stations for a DC fast charging application [1], [2]. In both mentioned applications, some main features are required such as high-power factor correction (PFC), high conversion efficiency, regulated low ripple output voltage, and electrical isolation for safety purposes. Mainstream three-phase rectifiers such as Vienna rectifier (boost-type) and Swiss rectifier (buck-type) require a second stage DC-DC converter for low ripple output voltage regulation and electrical isolation, which often imposes a reduced total conversion efficiency and power density [3], [4]. In such two-stage approaches, to reduce the total conversion efficiency, multi-phase soft-switching DC-DC converters like phase-shifted full-bridge converters and resonant converters are used as the second stage to provide voltage isolation and regulation [5]-[7].

On the other hand, single-stage rectifiers have gained a lot of attention in recent years as they can potentially achieve higher power density and efficiency than two-stage approaches [8]-[10]. Most three-phase converters require complex control implementation using DQ transformation, and some of them require a large number of passive components such as coupled inductors and DC-link capacitors. Another interesting solution for three-phase AC-DC converters is a phase-modular approach based on the existing knowledge of single-phase designs. In this method, one-third of the output power is processed in each phase so the conversion efficiency of the three-phase system is equivalent to the efficiency of a single-phase module. The phase-modular structure can be implemented with two stages [11]-[13], which usually demands relatively large DC-link capacitors on each phase and the power conversion efficiency is lower than single-stage approaches.

Different single-stage topologies have been investigated in the phase-modular designed three-phase AC-DC converter structure, active clamp boost converter in [14], flyback converter in [15], SEPIC converter in [16], Zeta converter in [17], Cuk converter in [18], full-bridge converter in [19], push-pull converter in [20]. In [21], a three-phase high power density rectifier is proposed based on a single-stage Dual Active Bridge (DAB) converter. In the proposed rectifier a new triple phase shift control is used to perform a proper PFC. In [22] and [23], a novel three-phase single-stage rectifier is proposed based on LLC, i.e., inductor (L), inductor (L), capacitor (C), resonant converter modules. The main interesting feature of the mentioned topologies is that all the knowledge of a single-phase converter can be expanded to the three-phase system suggesting less complexity in the design. Moreover, as the reactive power of the three-phase input is canceled out in the output there is no need for a large electrolytic capacitor, which increases the system reliability and power density. Most of the literature only discussed the implementation and power circuit performance in a balanced four-wire or three-wire three-phase system using inner current control loops to achieve PFC.

One main challenge for three-phase AC-DC converters is the presence of double line frequency output ripple in case of any imbalance in the three-phase input voltages. This problem comes from unbalanced power-sharing between the three phases due to unbalanced input voltages and using proportional/fixed

current reference signals for all phases. This issue is critical in single-stage AC-DC converters as there is no post-regulation DC-DC stage to reduce the low-frequency voltage ripple caused by unbalanced input voltages. Therefore, a power balancing circuit is a necessity for single-stage three-phase AC-DC converters to fully benefit from the small output capacitance feature.

Not so many research papers can be found in the literature concerning the impact of unbalances on phase-modular three-phase AC-DC converters. In [18], power balancing control is done based on inductor current calculation for each phase using input voltage, output voltage, and output current. The calculation of the inductor current resulted in the output voltage of the converter becoming independent of the variation in input voltage and DC load current. In [21], a simple power control balancing is implemented in a modular three-phase DAB AC-DC converter. This method reads the output current through a low pass filter on each phase and then creates a reference current based on the input voltage to do the power balancing, hence this method has slow dynamics and requires additional sensing circuits.

In this paper, a novel simple inner control method is proposed for three-phase single-stage AC-DC converters to do the PFC and power balancing at the same time without adding to the complexity of the system. In the presence of input voltage imbalances, the resulting double line frequency ripple in the output capacitor can be removed by the proposed instantaneous power balancing control while performing PFC, and hence the dynamic of the system is fast. The latter significantly reduces the output capacitance requirement and hence no electrolytic capacitor will be needed in three-phase single-stage AC-DC converters, which will significantly increase the system reliability. In the next section, the phase-modular three-phase AC-DC converter is analyzed with balanced and unbalanced conditions. The proposed control method is implemented for a phase-modular designed three-phase single-stage LLC-based AC-DC converter in Section III. Computer simulation and experimental results are provided in Section IV for performance verification, and the paper is concluded in Section V.

II. PHASE-MODULAR THREE-PHASE SINGLE-STAGE AC-DC CONVERTERS

Fig. 1 illustrates the general structure of phase-modular designed three-phase single-stage AC-DC converters. As discussed in the previous section, different converter modules can be used in each phase to perform the PFC. The input of each PFC module is a rectified AC voltage (v_{inA} , v_{inB} and v_{inC}) and hence the output voltage (v_{oA} , v_{oB} and v_{oC}) contains double line frequency voltage ripple. Since the three-phase AC input voltages have a fixed 120° displacement between each other, the double line frequency ripple gets canceled out in the output of the phase-modular three-phase AC-DC converter, which leads to a negligible output voltage ripple only containing the switching frequency ripple, so no bulky electrolytic capacitor is required. However, if the input voltages are unbalanced then a double line frequency ripple appears in the output voltage, which is undesirable.

Fig. 2 illustrates a single-stage LLC resonant converter module that can be used in the phase-modular three-phase AC-DC converter to perform PFC [22]. Since the LLC tank has a boost function in the inductive region, the voltage gain can be tuned by varying the switching frequency over the line cycle from the zero-crossing point to the peak AC voltage. In the design of a single-stage LLC converter for PFC application it is desired to keep the switching frequency (f_{sw}) range between the parallel resonant frequency (f_p) and series resonant frequency (f_s) to make sure both Zero Voltage Switching (ZVS) and Zero Current Switching (ZCS) can be achieved for the switches over the line cycle. Fig. 3 illustrates the gain curves of the LLC tank over the line cycle from double output power delivery at peak line voltage (i.e., $\theta=90^\circ$) to no output power delivery around the zero-voltage crossing (i.e., $\theta=0^\circ$). The main advantage of the LLC converter is that the switching loss is negligible due to soft-switching and hence the conversion loss becomes conduction loss only. Moreover, a high switching frequency can be implemented leading to an improved power density without compromising the conversion efficiency.

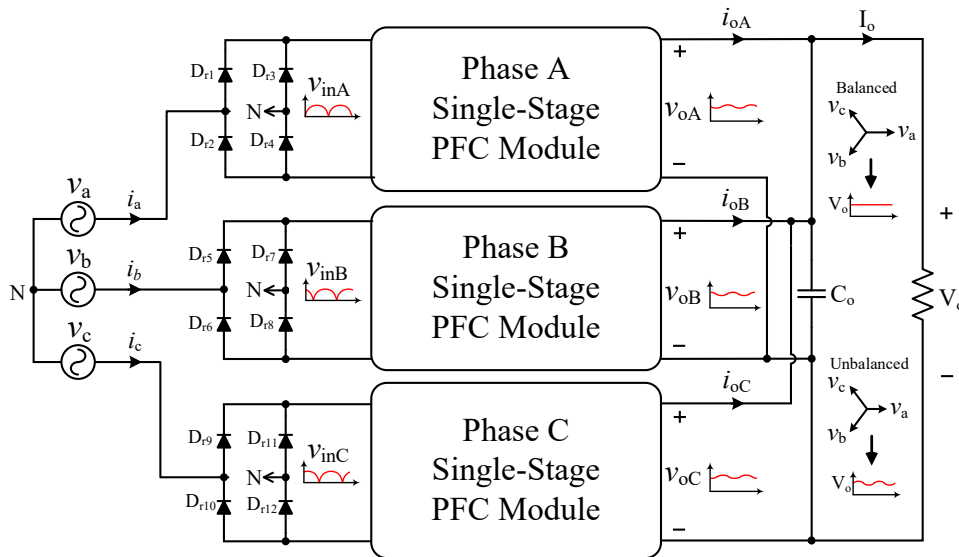


Fig. 1. The general structure of phase-modular designed three-phase single-stage AC-DC converter.

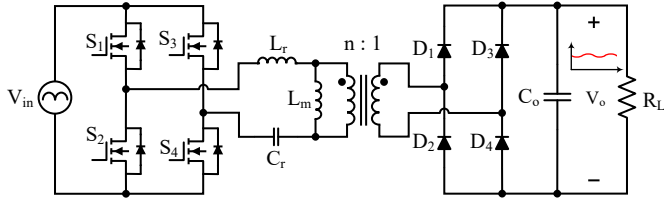


Fig. 2. A single-stage PFC module based on the full-bridge LLC resonant converter.

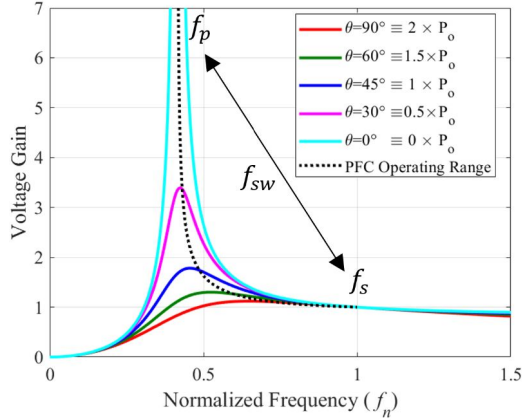


Fig. 3. Typical voltage gain curves of the single-stage LLC resonant converter over the half-line cycle PFC operation.

Assuming a pure sinusoidal current with a unity power factor for each phase, the voltage and current of the three-phase system can be written as follows.

$$\begin{cases} v_a = \sqrt{2}V_a \sin(\omega t) \\ v_b = \sqrt{2}V_b \sin(\omega t - 120^\circ) \\ v_c = \sqrt{2}V_c \sin(\omega t + 120^\circ) \end{cases} \quad (1)$$

$$\begin{cases} i_a = \sqrt{2}I_a \sin(\omega t) \\ i_b = \sqrt{2}I_b \sin(\omega t - 120^\circ) \\ i_c = \sqrt{2}I_c \sin(\omega t + 120^\circ) \end{cases} \quad (2)$$

where V_a, V_b and V_c are the Root Mean Square (RMS) value of grid voltages, I_a, I_b and I_c are the RMS value of AC input currents and ω is the line angular frequency. In the rest of this paper, subscript ‘‘a’’ or ‘‘A’’ denotes phase A parameters, subscript ‘‘b’’ or ‘‘B’’ denotes phase B parameters, and subscript ‘‘c’’ or ‘‘C’’ denotes phase C parameters. In a constant current controlled three-phase PFC converter, the RMS current is the same for a balanced condition, i.e., $I_a = I_b = I_c = I$, and $V_a \neq V_b \neq V_c$ for an unbalanced grid voltage condition. The analysis of the creation of double-line frequency in total output current and voltage is provided as follows. The instantaneous three-phase input power can be calculated for unbalanced grid conditions using (1) and (2) as follows.

$$p_{3ph} = v_a \times i_a + v_b \times i_b + v_c \times i_c = P_{in} + P_{2\omega} \cos(2\omega t) \quad (3)$$

In the above equation, P_{in} is the average input power and $P_{2\omega}$ is the amplitude of the double line frequency of pulsating power that is expressed in (4) and (5), respectively.

$$P_{in} = V_a I + V_b I + V_c I \quad (4)$$

$$P_{2\omega} \cos(2\omega t) = -V_a I \cos(2\omega t) - V_b I \cos(2\omega t - 240^\circ) - V_c I \cos(2\omega t + 240^\circ) \quad (5)$$

From (5) it can be seen that with a balanced three-phase voltage the pulsating part of the output power gets canceled out. The rectified current in each phase has an average value plus a high-frequency term. Assuming the switching frequency is very large, and the energy stored in the output capacitor is negligible, then the instantaneous input power equals the instantaneous output power for a lossless circuit. Hence, the high-frequency term of the rectified current is neglected, and the average output current of each phase can be written as follows.

$$i_{oA} = \frac{v_a i_a}{V_o}, \quad i_{oB} = \frac{v_b i_b}{V_o}, \quad i_{oC} = \frac{v_c i_c}{V_o} \quad (6)$$

where V_o is the average output voltage that is considered to be DC. Hence, the instantaneous output current which is the sum of three-phase output currents can be expressed as follows.

$$i_o = i_{oA} + i_{oB} + i_{oC} = I_o + I_{2\omega} \cos(2\omega t) \quad (7)$$

In the above equation, I_o is the average output current (DC part) and $I_{2\omega}$ is the amplitude of the double line frequency component of pulsating current that is expressed in (8) and (9), respectively.

$$I_o = \frac{V_a I}{V_o} + \frac{V_b I}{V_o} + \frac{V_c I}{V_o} \quad (8)$$

$$I_{2\omega} \cos(2\omega t) = -\frac{V_a I}{V_o} \cos(2\omega t) - \frac{V_b I}{V_o} \cos(2\omega t - 240^\circ) - \frac{V_c I}{V_o} \cos(2\omega t + 240^\circ) \quad (9)$$

In the above equation, if the amplitude of three-phase input voltages is not the same, the double line frequency pulsating current term cannot be canceled, and hence the output current and output voltage will have the double line frequency ripple.

Fig. 4 illustrates the per unit input AC voltages (v_a, v_b, v_c) and per unit AC currents (i_a, i_b, i_c), and instantaneous power of each phase (p_a, p_b, p_c) as well as total three-phase power (p_{3ph}) for an unbalanced condition with the initially balanced operation. A 10% step decrease in the voltage of phase A and a 5% step increase in the voltage of phase B and phase C occurred at the time of 25 ms in Fig. 4. To keep the total three-phase power at unity, the sum of step increase and step decrease in input voltages are equal. As can be observed from the bottom row of Fig. 4 as soon as the input voltages get unbalanced the total per unit three-phase power is not purely DC anymore and a pulsating double line frequency term has created that passes through the output capacitor.

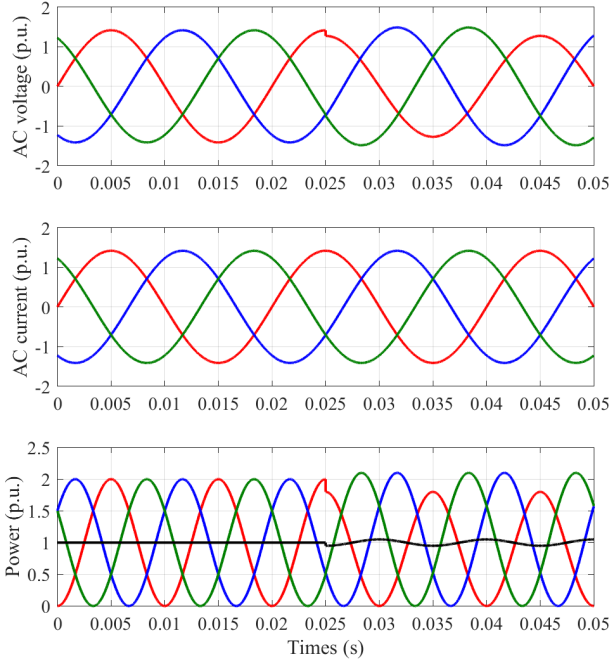


Fig. 4. The per unit representation of three-phase AC input voltages (v_a , v_b , v_c), currents (i_a , i_b , i_c), and instantaneous power of each module (p_a , p_b , p_c) as well as the total three-phase power (p_{3ph}). Red color denotes phase A, blue color denotes phase B, and green color denotes phase C.

III. THE PROPOSED POWER BALANCING CONTROL METHOD FOR THREE-PHASE SINGLE-STAGE AC-DC CONVERTERS

As discussed in the previous section, any imbalance in the amplitude of the three input AC sources leads to the presence of a double line frequency ripple in the output of phase-modular three-phase AC-DC converters. To solve this problem, instantaneous power balancing is proposed using power reference signals for each phase instead of current reference signals. In this way, as the input voltages are sinusoidal the input currents will be indirectly controlled to be sinusoidal. This method allows the power distribution between the three phases to be always balanced and hence no double line frequency ripple will be reflected into the output. In this method, the input voltage and current are sensed to perform the PFC and power balancing control at the same time, so no complexity or cost is added to the original circuit with conventional fixed current control methods.

In order to cancel out the double line frequency ripple in the output current, the current reference of each phase should change such that the multiplication of each phase's voltage and current are identical in all terms of (9), so the fluctuating current

can be canceled. Ignoring the power losses, the average input power is equal to the average output power in each phase (i.e., $P_{inj} = P_{oj}$ where $j=A, B, C$), so the relationship between the instantaneous input power and average output power in each phase can be written as follows.

$$\begin{cases} p_{inA} = P_{oA}(1 - \cos(2\omega t)) \\ p_{inB} = P_{oB}(1 - \cos(2\omega t - 240^\circ)) \\ p_{inC} = P_{oC}(1 - \cos(2\omega t + 240^\circ)) \end{cases} \quad (10)$$

Considering a pure sinusoidal grid voltage, if the input power of each phase is controlled to satisfy (10), a high power factor can be achieved in each phase and at the same time the average output power of each phase will be indirectly controlled to be identical in all three phases (i.e. $P_{oA} = P_{oB} = P_{oC} = P_o/3$). In the outer voltage control loop, the output of a PI compensator is a power control signal (P_{ctrl}) that regulates the output voltage level. Hence, the reference power for each phase can be expressed as follows.

$$\begin{cases} p_{refA} = P_{ctrl}(1 - \cos(2\omega t)) \\ p_{refB} = P_{ctrl}(1 - \cos(2\omega t - 240^\circ)) \\ p_{refC} = P_{ctrl}(1 - \cos(2\omega t + 240^\circ)) \end{cases} \quad (11)$$

If the input voltage is polluted with harmonics, then depending on the amount of voltage distortion the maximum achievable power factor is going to be below unity. The maximum amount of allowable Total Harmonics Distortion (THD) for general purposes is 5% based on IEEE 519-1992 standard [24]. The input AC voltages can be represented as in (12) if some odd harmonics are considered (e.g., 3rd and 5th, etc.). In (12), V_{k1} , V_{k3} and V_{k5} (where $k=a, b$, and c) are the RMS value of first, third, and fifth voltage harmonics, respectively. To compare the instantaneous power with the reference signal that has a DC component plus a double line frequency component, the multiplication of three-phase voltages and currents should have only the mentioned two components as shown in (3). A solution that allows higher-order harmonics cancellation in the instantaneous power is that the resulting input current has the same harmonics content in the grid voltage, but with the opposite sign. Hence, for the proposed power-controlled PFC, the resulting current waveforms considering harmonics presented in (12) can be represented as (13). In (13), I_{k1} , I_{k3} and I_{k5} (where $k=a, b$, and c) are the RMS value of first, third, and fifth current harmonics, respectively.

Fig. 5 illustrates the per unit representation of three-phase input voltages with the addition of some odd harmonics totaling 5 % THD as well as input currents with the same harmonic

$$\begin{cases} v_a = \sqrt{2}V_{a1} \sin(\omega t) + \sqrt{2}V_{a3} \sin(3\omega t) + \sqrt{2}V_{a5} \sin(5\omega t) + \dots \\ v_b = \sqrt{2}V_{b1} \sin(\omega t - 120^\circ) + \sqrt{2}V_{b3} \sin(3\omega t) + \sqrt{2}V_{b5} \sin(5\omega t + 120^\circ) + \dots \\ v_c = \sqrt{2}V_{c1} \sin(\omega t + 120^\circ) + \sqrt{2}V_{c3} \sin(3\omega t) + \sqrt{2}V_{c5} \sin(5\omega t - 120^\circ) + \dots \end{cases} \quad (12)$$

$$\begin{cases} i_a = \sqrt{2}I_{a1} \sin(\omega t) - \sqrt{2}I_{a3} \sin(3\omega t) - \sqrt{2}I_{a5} \sin(5\omega t) - \dots \\ i_b = \sqrt{2}I_{b1} \sin(\omega t - 120^\circ) - \sqrt{2}I_{b3} \sin(3\omega t) - \sqrt{2}I_{b5} \sin(5\omega t + 120^\circ) - \dots \\ i_c = \sqrt{2}I_{c1} \sin(\omega t + 120^\circ) - \sqrt{2}I_{c3} \sin(3\omega t) - \sqrt{2}I_{c5} \sin(5\omega t - 120^\circ) - \dots \end{cases} \quad (13)$$

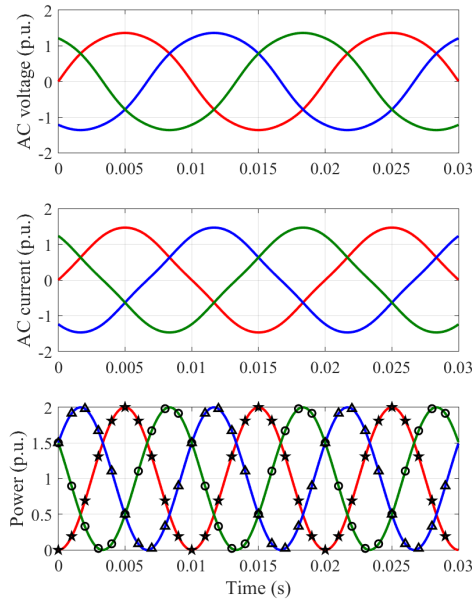


Fig. 5. Three-phase input voltages, currents, and powers considering some harmonics in the grid voltages using the proposed instantaneous power balancing control method.

content with opposite sign. The resulting instantaneous power is shown with solid lines in the bottom row of Fig. 5 and the markers are from plotting (10). It can be observed that the markers are perfectly aligned on solid lines, which proves that only the second harmonic has remained in the instantaneous power. With fixed power control, if there is any harmonic in grid voltages there will be the same harmonic content with the negative sign in the current. Based on the definition, THD is the ratio of the square root of the sum of the RMS value square of all harmonic components over the RMS value square of the first harmonic, which is insensitive to the sign of harmonics. Hence, the same amount of THD in AC voltage is supposed to be projected in the AC current as well. It should be mentioned that the PFC converter itself can have some sort of current distortion in different scenarios that are not considered here. Hence, considering a unity PFC performance for the AC-DC converter, the maximum achievable power factor with the proposed instantaneous power control in the presence of harmonics in the grid voltages (THD_v) can be calculated as follows.

$$PF = \frac{1}{1 + THD_v^2} \quad (14)$$

With 5% THD in grid voltages, the maximum achievable power factor would be 0.9975 with the proposed power control. In comparison, with constant current control, the maximum achievable power factor would be 0.9987. As long as the PFC operation of the AC-DC converter is near unity and the grid voltage harmonic contents are within standards, the difference occurred in power factor due to voltage harmonics is negligible between the proposed instantaneous power balancing control method and conventional constant current control method.

The digital implementation of the proposed instantaneous power control scheme is depicted in Fig. 6. As can be observed, the input voltage and current are sampled to calculate the

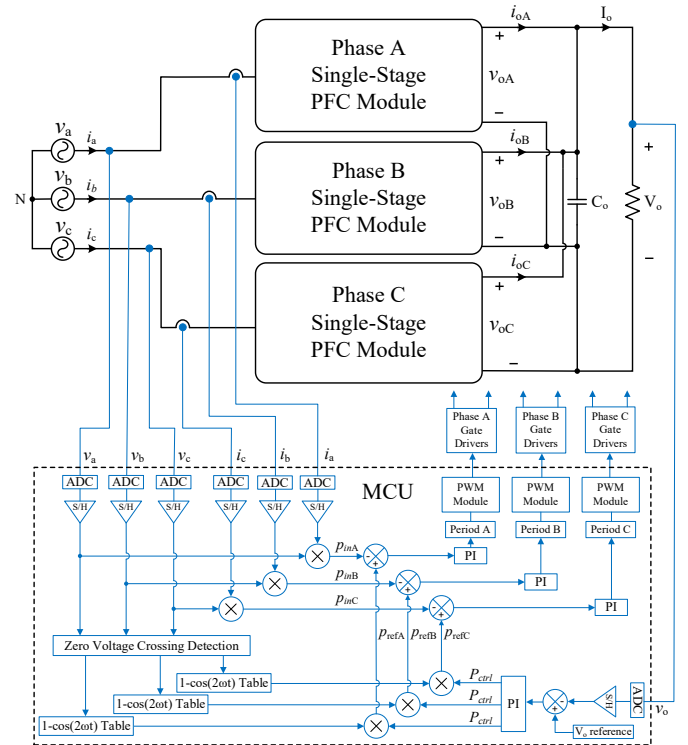


Fig. 6. Digital implementation of the proposed PFC and power balancing control method for phase-modular designed three-phase single-stage AC-DC converters.

instantaneous input power of each phase (i.e., p_{inj} where $j=A, B, C$). Moreover, input voltage zero-crossing detection is used to generate synchronized $1 - \cos(2\omega t)$ signals using look-up tables for each phase that creates the reference power signals for each phase (i.e., p_{refj} where $j=A, B, C$) using the power control signal (i.e., P_{ctrl}) coming from the outer voltage loop, which is then compared with the respective p_{inj} signals. Later, the error signals are fed into three independent PI controllers to create the period for modulating the LLC converter modules.

IV. SIMULATION AND EXPERIMENTAL RESULTS

To verify the performance of the proposed power balancing control method a three-phase single-stage LLC-based AC-DC converter is implemented in the PSIM environment. Both conventional constant current control and the proposed instantaneous power balancing control method are implemented for comparison purposes. The RMS value of input AC voltage is 220 V at 50 Hz, and the output DC voltage range is from 250 V to 380 V similar to the design discussed in [22]. The switching frequency range is from 200 kHz to 450 kHz. The rated output power is 1.5 kW and the output capacitor is a 60 μ F Film capacitor. The input voltage and current are sensed for the fast inner loop to realize PFC using both the conventional constant current control and proposed instantaneous power control methods, and the output voltage is sensed for output voltage regulation.

Fig. 7 illustrates the simulation results with the conventional constant current control method. First, all the three-phase input voltages are balanced and at a time of 80 ms, the amplitude of phase A is reduced by 15%. Fig. 7(a) illustrates the $V_o=250$ V

and $P_o=1$ kW condition. It can be observed that the output voltage ripple is small in balanced operation, however, after input voltage imbalance the output voltage has a double line frequency peak-to-peak voltage ripple of around 5.5 V. Moreover, it can be observed that the power factor is near unity, and the input current THD₁ is around 1.6 % for this load condition. Fig. 7(b) illustrates the $V_o=380$ V and $P_o=1.5$ kW condition. It can be observed that after the input voltage imbalance condition the peak-to-peak output voltage ripple is as large as 8V which is more than 20 times the balanced input voltage condition. Moreover, the input current THD₁ is around 1 % for this condition. Hence, implementing a power balancing control is necessary to keep the voltage ripple as well as the stress on the output capacitor low.

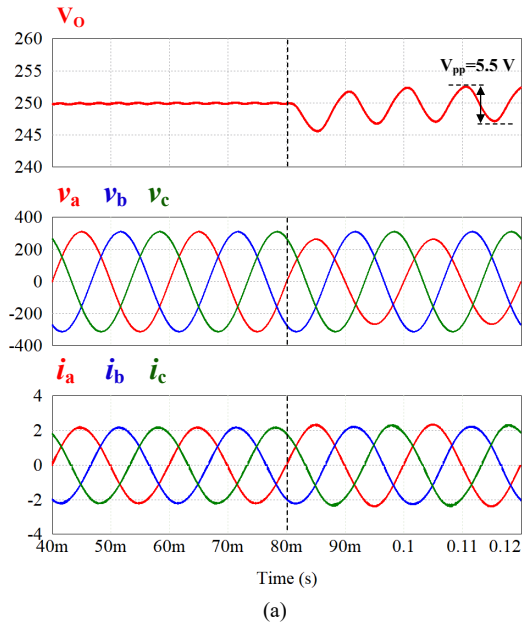


Fig. 8(a) and (b) illustrate the proposed instantaneous power balancing control method for the same input voltage imbalance for two different output voltage and power conditions. It can be observed that the input current in both cases remains sinusoidal with near-unity power factor operation. It can be observed that the dynamic of the system is fast with the proposed instantaneous power control method and there is no low-frequency voltage ripple in the output voltage during the step change in the AC input voltage. Moreover, the input current THD₁ is around 2.5 % for $V_o=250$ V condition and it is around 1.8 % for $V_o=380$ V condition. There is a short flat part near the line voltage zero-crossings that is mainly because of using the same sensing and PI parameters for both methods while the

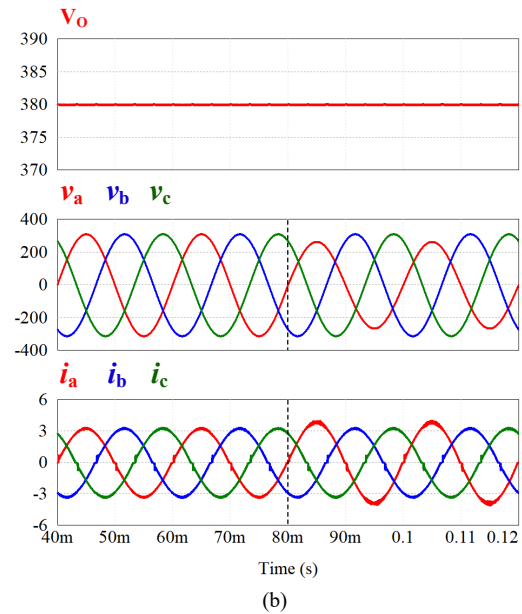
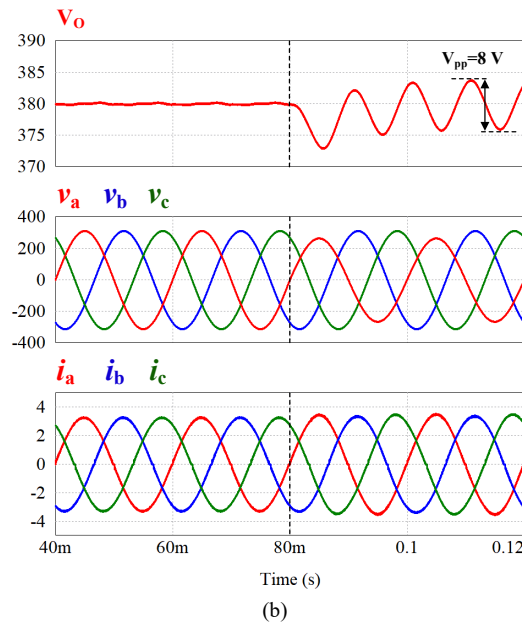
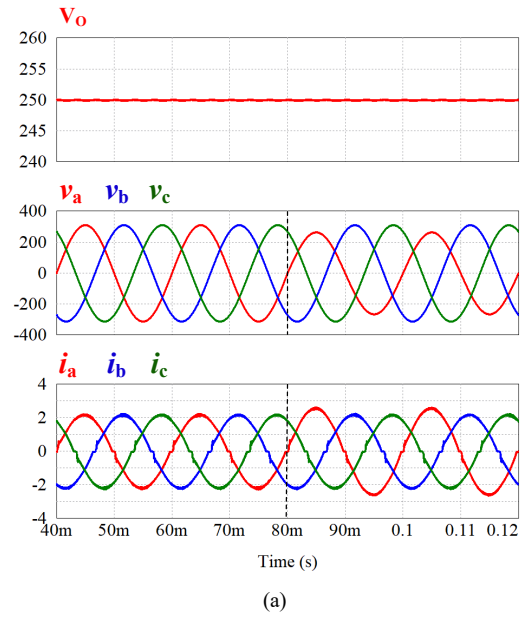


Fig. 8. Simulation results of the three-phase single-stage LLC-based AC-DC converter with conventional constant current control for (a) $V_o=250$ V and $P_o=1$ kW, and (b) $V_o=380$ V and $P_o=1.5$ kW.

Fig. 7. Simulation results of the three-phase single-stage LLC-based AC-DC converter with the proposed instantaneous power balancing control for (a) $V_o=250$ V and $P_o=1$ kW, and (b) $V_o=380$ V and $P_o=1.5$ kW.

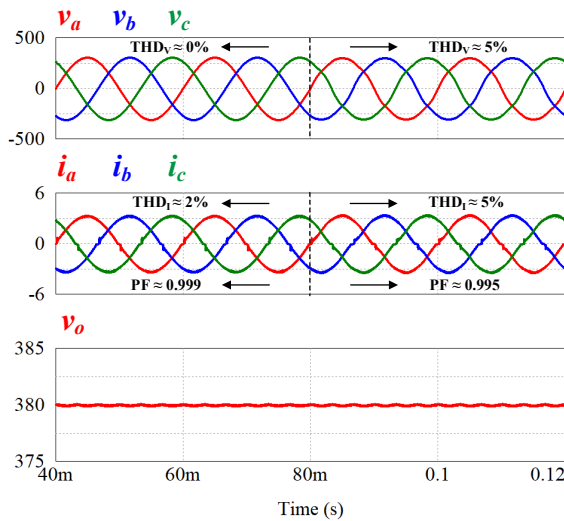


Fig. 9. Simulation results with the proposed instantaneous power balancing control reference signal at $V_o=380$ V, $P_o=1.5$ kW with harmonic polluted input three-phase voltages.

slope of the power reference signal is much slower than the current reference signal around the line voltage zero-crossing.

In order to check the performance of the proposed instantaneous power control method under a harmonic polluted grid, some voltage harmonics are added to the input voltage source to verify the power factor performance. Fig. 9 illustrates the simulation results with initially clean balanced three-phase grid voltages and harmonic polluted grid voltages after the time of 80 ms. From Fig. 9 it can be observed that in the presence of 5 % THD_v there is the same amount of harmonics in the input current and a near unity power factor of more than 0.99 is achieved with both purely first harmonic and with added higher-order harmonics in the three-phase input voltages.

The proposed instantaneous power balancing control is implemented in a single dsPIC microcontroller to be used with the 1.5 kW three-phase LLC-based laboratory prototype described in [22]. The input current of the LLC resonant converter module is sensed through a sensing resistor that is then multiplied with the sampled input voltage of each phase to calculate the instantaneous input power. To generate the reference power signals, a look-up table is called starting at the voltage zero-crossing points of the input voltages. The output voltage is sampled and compared to a reference voltage and then is passed through a digital PI compensator to generate the proper amplitude of the power control signal that multiplies with respective $1-\cos(2\omega t)$ term for each phase. Therefore, three independent time-varying reference power signals are generated based on the input power of each phase that can be compared with the sensed instantaneous input power signals. Then, the error signals are passed through three inner digital PI compensators to generate proper periods for the dedicated PWM modules for phases A, B, and C. Hence, in the proposed control method, there is one outer voltage loop to realize output voltage regulation, and there are three inner power control loops to realize PFC and power balancing at the same time. Hence, the dynamic of the system is fast, and the double line frequency output voltage ripple will not be large even during transients.

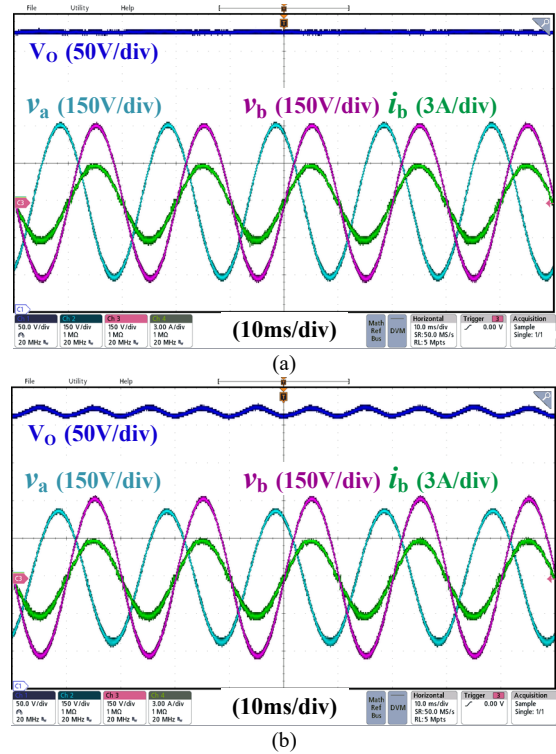


Fig. 10. Experimental results with the conventional current control with a fixed current reference signal for $V_o=380$ V, $P_o=1.5$ kW, (a) with a balanced three-phase input voltage (i.e., $V_a=V_b=V_c=220$ V_{RMS}), and (b) with unbalanced three-phase input voltage (i.e., $V_a=190$ V_{RMS}, $V_b=V_c=220$ V_{RMS}).

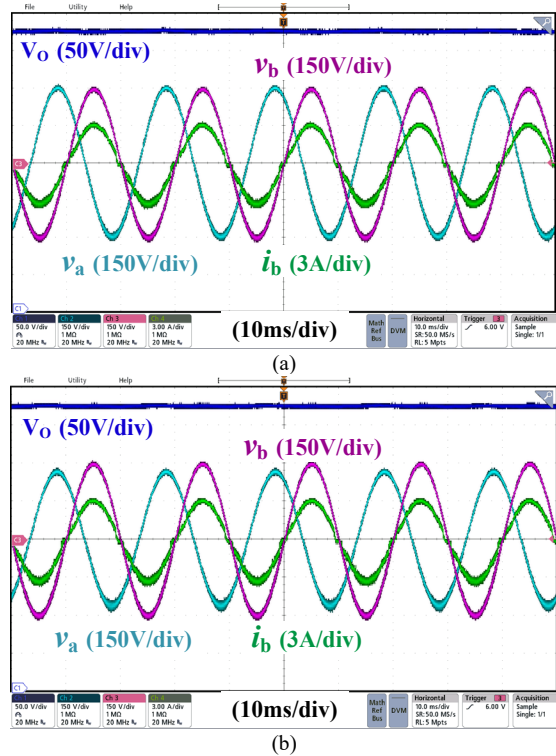


Fig. 11. Experimental results with the proposed instantaneous power balancing control method for $V_o=380$ V, $P_o=1.5$ kW, (a) with a balanced three-phase input voltage (i.e., $V_a=V_b=V_c=220$ V_{RMS}), and (b) with unbalanced three-phase input voltage (i.e., $V_a=190$ V_{RMS}, $V_b=V_c=220$ V_{RMS}).

Fig. 10(a) illustrates the experimental results for $V_o=380$ V and $P_o=1.5$ kW with the conventional constant current control method and balanced input voltages. It can be observed that the input current is sinusoidal with a low THD and the output voltage does not contain any low-frequency voltage ripple. From Fig. 10(b) it can be observed that after reducing the voltage of phase A from 220V to 190V the output voltage contains a double line frequency ripple that is more than 15 V peak-to-peak. Fig. 11(a) and (b) illustrate the proposed instantaneous power balancing control with balanced and unbalanced input voltages, respectively. It can be observed that in both cases the power factor is near unity and the output voltage ripple does not carry any low-frequency voltage ripple. The experimental results are in accordance with the computer simulations.

V. CONCLUSION

A new instantaneous power balancing control method is proposed for phase-modular three-phase single-stage AC-DC converters. Both the PFC and power balancing are done at the same time and hence the system dynamics are fast in transients. The proposed power control method does not use additional sensing circuits to perform power balancing as compared with the conventional constant current control method which requires additional sensing and control loops. Simulation results of a three-phase single-stage LLC-based AC-DC converter with both balanced and unbalanced three-phase voltages verified the double line frequency ripple rejection and fast transient response of the proposed power control. Moreover, the digital implementation of the proposed control method on a laboratory prototype demonstrated the efficacy of the proposed method in both balanced and unbalanced conditions. It is shown that using the proposed power balancing control method, the output capacitance requirement of the three-phase single-stage LLC-based AC-DC converter has remained small even in the presence of unbalanced input voltages which allowed film capacitor implementation. Furthermore, a high-power factor (i.e. >0.99) has been achieved with the proposed power control method with both balanced and unbalanced three-phase input voltage conditions with and without input voltage harmonics.

REFERENCES

- [1] R. Girod and D. Weida, "High Efficient True 3-Phase Compact Switch-Mode Rectifier Module for Telecom Power Solutions," in *IEEE Proc. INTELEC*, Hamburg, Germany, 2013, pp. 1-6.
- [2] K. Yoo, K. Kim and J. Lee, "Single- and Three-Phase PHEV Onboard Battery Charger Using Small Link Capacitor," *IEEE Trans. Ind. Electron.*, vol. 60, no. 8, pp. 3136-3144, Aug. 2013.
- [3] J. A. Anderson, M. Haider, D. Bortis, J. W. Kolar, and M. Kasper, "New Synergetic Control of a 20kW Isolated VIENNA Rectifier Front-End EV Battery Charger," in *IEEE Proc. COMPEL*, Toronto, ON, 2019, pp. 1-8.
- [4] T. B. Soeiro, T. Friedli and J. W. Kolar, "Swiss rectifier — A novel three-phase buck-type PFC topology for Electric Vehicle battery charging," in *IEEE Proc. APEC*, Orlando, FL, 2012, pp. 2617-2624.
- [5] Y. Cui, W. Zhang, L. M. Tolbert, D. J. Costinett, F. Wang and B. J. Blalock, "Two phase interleaved ISOP connected high step down ratio phase shift full bridge DC/DC converter with GaN FETs," in *IEEE Proc. APEC*, 2015, pp. 1414-1419.
- [6] R. Gadelrab, F. C. Lee and Q. Li, "Three-Phase Interleaved LLC Resonant Converter with Integrated Planar Magnetics for Telecom and Server Application," in *IEEE Proc. APEC*, 2020, pp. 512-519.

- [7] M. Forouzesh and Y. -F. Liu, "Interleaved LCLC Resonant Converter With Precise Current Balancing Over a Wide Input Voltage Range," *IEEE Trans. Power Electron.*, vol. 36, no. 9, pp. 10330-10342, Sept. 2021.
- [8] D. Das, N. Weise, K. Basu, R. Baranwal and N. Mohan, "A Bidirectional Soft-Switched DAB-Based Single-Stage Three-Phase AC-DC Converter for V2G Application," *IEEE Trans. Transport. Electrific.*, vol. 5, no. 1, pp. 186-199, March 2019.
- [9] K. Ali, S. K. Dube, P. Das, and J. C. Peng, "Improvement of ZVS Range and Current Quality of the Nine-Switch Single-Stage AC-DC Converter," *IEEE Trans. Power Electron.*, vol. 35, no. 5, pp. 4658-4668, May 2020.
- [10] K. Shigeuchi, J. Xu, N. Shimosato and Y. Sato, "A Modulation Method to Realize Sinusoidal Line Current for Bidirectional Isolated Three-Phase AC/DC Dual-Active-Bridge Converter Based on Matrix Converter," *IEEE Trans. Power Electron.*, vol. 36, no. 5, pp. 6015-6029, May 2021.
- [11] M. L. Heldwein, A. Ferrari de Souza and I. Barbi, "A simple control strategy applied to three-phase rectifier units for telecommunication applications using single-phase rectifier modules," in *IEEE Proc. PESC*, Charleston, SC, USA, 1999, pp. 795-800 vol.2
- [12] H. Kim, J. Baek, M. Ryu, J. Kim and J. Jung, "The High-Efficiency Isolated AC-DC Converter Using the Three-Phase Interleaved LLC Resonant Converter Employing the Y-Connected Rectifier," *IEEE Trans. Power Electron.*, vol. 29, no. 8, pp. 4017-4028, Aug. 2014.
- [13] G. Yang, E. Draugedalen, T. Sorsdahl, H. Liu and R. Lindseth, "Design of High Efficiency High Power Density 10.5kW Three Phase On-board-charger for Electric/hybrid Vehicles," in *Proc. PCIM Europe*, Nuremberg, Germany, 2016, pp. 1-7.
- [14] H. M. Suryawanshi, M. R. Ramteke, K. L. Thakre and V. B. Borghate, "Unity-Power-Factor Operation of Three-Phase AC-DC Soft Switched Converter Based On Boost Active Clamp Topology in Modular Approach," *IEEE Trans. Power Electron.*, vol. 23, no. 1, pp. 229-236, Jan. 2008.
- [15] B. Tamyurek and D. A. Torrey, "A Three-Phase Unity Power Factor Single-Stage AC-DC Converter Based on an Interleaved Flyback Topology," *IEEE Trans. Power Electron.*, vol. 26, no. 1, pp. 308-318, Jan. 2011.
- [16] G. Tibola and I. Barbi, "Isolated Three-Phase High Power Factor Rectifier Based on the SEPIC Converter Operating in Discontinuous Conduction Mode," *IEEE Trans. Power Electron.*, vol. 28, no. 11, pp. 4962-4969, Nov. 2013.
- [17] B. Singh, S. Singh and G. Bhuvanwswari, "Analysis and Design of a Zeta Converter Based Three-Phase Switched Mode Power Supply," in *Proc. CICON, Mathura*, 2012, pp. 571-575.
- [18] U. Kamnam and V. Chunkag, "Analysis and Design of a Modular Three-Phase AC-to-DC Converter Using CUK Rectifier Module With Nearly Unity Power Factor and Fast Dynamic Response," *IEEE Trans. on Power Electron.*, vol. 24, no. 8, pp. 2000-2012, Aug. 2009.
- [19] G. Bhuaneswari, S. Narula and B. Singh, "Three-phase push-pull modular converter based welding power supply with improved power quality," in *Proc. IICPE*, Delhi, 2012, pp. 1-5.
- [20] Y. K. E. Ho, S. Y. R. Hui and Yim-Shu Lee, "Characterization of single-stage three-phase power-factor-correction circuit using modular single-phase PWM DC-to-DC converters," *IEEE Trans. Power Electron.*, vol. 15, no. 1, pp. 62-71, Jan. 2000.
- [21] J. Lu, K. Bai, A. R. Taylor, G. Liu, A. Brown, P. M. Johnson and M. McAmmond, "A Modular-Designed Three-Phase High-Efficiency High-Power-Density EV Battery Charger Using Dual/Triple-Phase-Shift Control," *IEEE Trans. Power Electron.*, vol. 33, no. 9, pp. 8091-8100, Sept. 2018.
- [22] M. Forouzesh, Y. -F. Liu and P. C. Sen, "Implementation of an Isolated Phase-Modular-Designed Three-Phase PFC Rectifier Based on Single-Stage LLC Converter," in *IEEE Proc. ECCE*, 2021, pp. 2266-2273.
- [23] M. Forouzesh, Y. -F. Liu and P. C. Sen, "A Novel Soft-Switched Three-Phase Three-Wire Isolated AC-DC Converter With Power Factor Correction," in *IEEE Proc. APEC*, 2022, pp. 887-894.
- [24] IEEE 519 Working Group. "IEEE recommended practices and requirements for harmonic control in electrical power systems." IEEE STD 519-1992, 1992.